Voltage-Dependent Calcium Channels at the Plasma Membrane, but Not Vesicular Channels, Couple Exocytosis to Endocytosis

Lei Xue,[1,2] Zhen Zhang,[1,2] Benjamin D. McNeil,[1] Fujun Luo,[1] Xin-Sheng Wu,[1] Jiansong Sheng,[1] Wonchul Shin,[1] and Ling-Gang Wu[1,*]

[1]National Institute of Neurological Disorders and Stroke, 35 Convent Drive, Building 35, Room 2B-1012, Bethesda, MD 20892, USA
[2]These authors contributed equally to this work
*Correspondence: wul@ninds.nih.gov
DOI 10.1016/j.celrep.2012.04.011

SUMMARY

Although calcium influx triggers endocytosis at many synapses and non-neuronal secretory cells, the identity of the calcium channel is unclear. The plasma membrane voltage-dependent calcium channel (VDCC) is a candidate, and it was recently proposed that exocytosis transiently inserts vesicular calcium channels at the plasma membrane, thus triggering endocytosis and coupling it to exocytosis, a mechanism suggested to be conserved from sea urchin to human. Here, we report that the vesicular membrane, when inserted into the plasma membrane upon exocytosis, does not generate a calcium current or calcium increase at a mammalian nerve terminal. Instead, VDCCs at the plasma membrane, including the P/Q-type, provide the calcium influx to trigger rapid and slow endocytosis and, thus, couple endocytosis to exocytosis. These findings call for reconsideration of the vesicular calcium channel hypothesis. They are likely to apply to many synapses and non-neuronal cells in which VDCCs control exocytosis, and exocytosis is coupled to endocytosis.

INTRODUCTION

Endocytosis is coupled to exocytosis, allowing recycling of vesicles and maintaining exocytosis (Royle and Lagnado, 2003; Schweizer and Ryan, 2006). Many studies suggest that calcium influx regulates endocytosis at synapses and non-neuronal secretory cells (Marks and McMahon, 1998; Cousin and Robinson, 1998; Gad et al., 1998; Sankaranarayanan and Ryan, 2001; Balaji et al., 2008; Artalejo et al., 1995; Neves et al., 2001; Wu et al., 2005; Clayton et al., 2007; but see von Gersdorff and Matthews, 1994; Leitz and Kavalali, 2011). Recent studies of a large nerve terminal, the calyx of Held, suggest that regulation of endocytosis by calcium reflects the trigger of endocytosis (Wu et al., 2009; Hosoi et al., 2009). Although the calcium channel that couples exo- to endocytosis was not identified, the voltage-dependent calcium channel (VDCC) was often implicitly assumed to be the candidate because calcium influx via VDCCs

triggers exocytosis, and exocytosis is coupled to endocytosis. However, a recent study of Drosophila synapses proposed that the calcium channel is Flower, a vesicular membrane protein transferred from the vesicle to the plasma membrane via vesicle fusion (Yao et al., 2009). This proposal may have significant impact for four reasons indicated by many reviews (Yao et al., 2009; Brose and Neher, 2009; Shupliakov and Brodin, 2010; Vogel, 2009; Kuo and Trussell, 2009). First, it could be a universal mechanism because Flower is conserved from worm to human (Yao et al., 2009). Second, experiments suggesting that calcium regulates or triggers endocytosis were mostly done by manipulating extracellular calcium or intracellular calcium buffers, which could be accounted for with the Flower hypothesis. Although the calcium current charge was found to correlate with the endocytosis rate (Wu et al., 2009), the exocytosis amount was not well controlled, making it possible for the vesicular calcium channel to account for this correlation. Thus, in principle, Flower could replace the plasma membrane VDCC to trigger endocytosis. Third, the Flower hypothesis explains exo-endocytosis coupling better than plasma membrane VDCCs because (1) Flower channels inserted to the plasma membrane may keep track of the level of exocytosis and thus be responsible for the exo-endocytosis match, and (2) Flower channels could diffuse to the endocytic zone, explaining why endocytic zones may differ from active zones. Fourth, a study in sea urchin eggs found that upon exocytosis, VDCCs are translocated from the vesicle membrane to the plasma membrane to mediate calcium influx required for endocytosis (Smith et al., 2000). These studies led to a more general hypothesis that vesicular calcium channels conserved from sea urchins to nerve terminals couple exo- to endocytosis (Vogel, 2009).

The vesicular channel hypothesis is potentially critical not only in exo-endocytosis coupling but also in many other calcium-dependent exocytosis processes (Brose and Neher, 2009; Kuo and Trussell, 2009). Despite such potential roles, whether fusion-inserted vesicle membrane generates calcium currents or influx at nerve terminals was not tested directly at nerve terminals. Whether plasma membrane VDCCs participate in triggering endocytosis with vesicular calcium channels is also unclear. The present work addressed these issues at the calyx of Held nerve terminal. We found that fusion-inserted vesicle membrane did not generate calcium currents or influx. Instead, the VDCC at nerve terminal membrane coupled exo- to endocytosis.
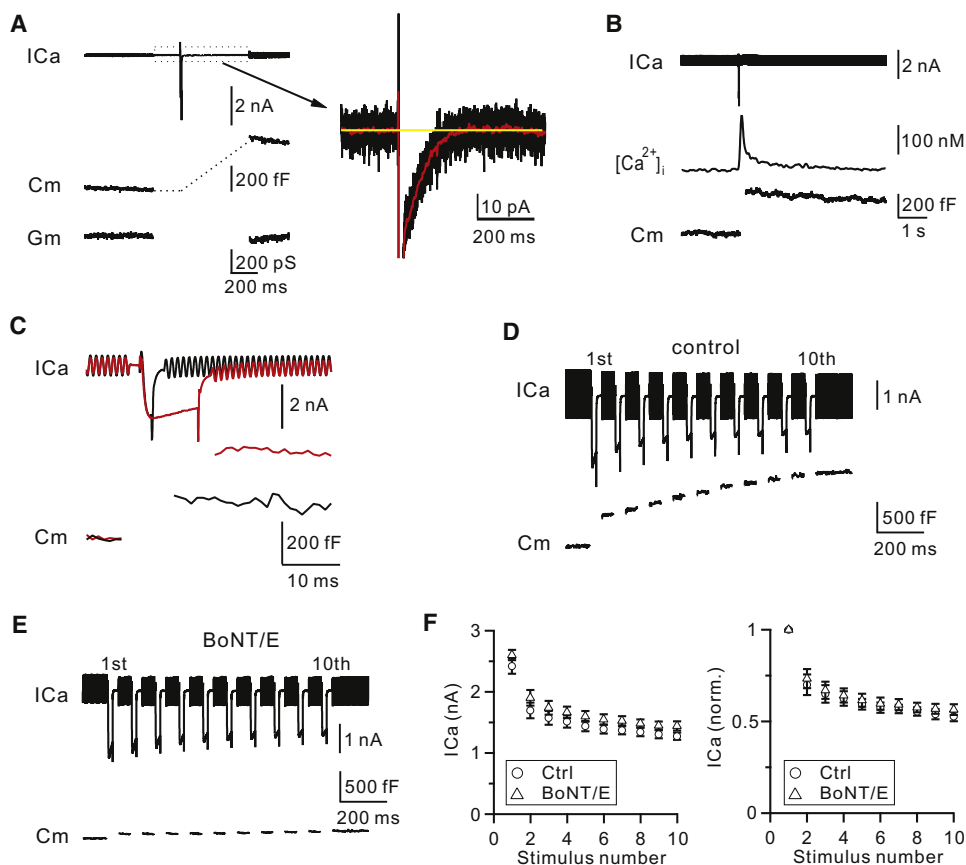
Figure 1. Vesicle Fusion Does Not Generate Calcium Currents at Nerve Terminals

(A) Left view shows sampled ICa, Cm, and Gm (membrane conductance) induced by a depol$_{10ms}$. ICa was low-pass filtered at 3 kHz. Right view presents ICa from the left view plotted in larger vertical and time scales (black). The red trace was the black trace low-pass filtered at 100 Hz. Yellow line is the mean baseline value.

(B) Sampled ICa, $[Ca^{2+}]_i$ and Cm induced by a depol$_{10ms}$.

(C) Sampled ICa and Cm induced by 2 (black) and 10 ms (red) depolarization.

(D and E) Sampled ICa and Cm induced by a depol$_{20ms \times 10}$ with a pipette containing 150 nM boiled BoNT/E (D, control) or BoNT/E (E).

(F) ICa (mean ± SE, left) and normalized ICa (right) induced by each 20 ms pulse during depol$_{20ms \times 10}$ in the presence of 150 nM boiled BoNT/E (circles) or BoNT/E (triangles).

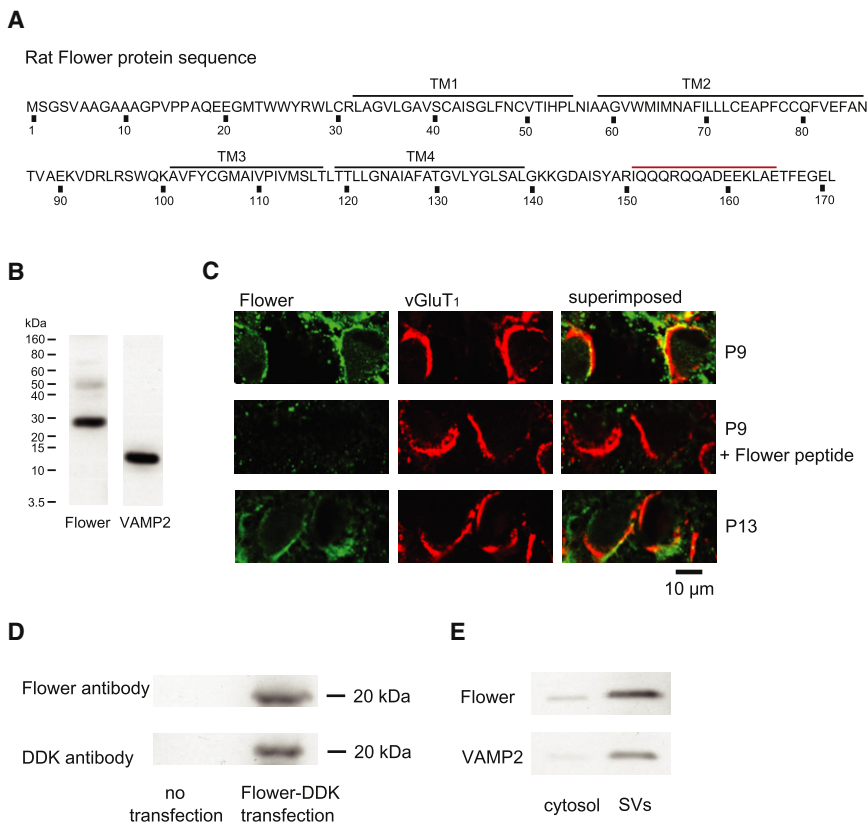See also Figures S1 and S2A.

RESULTS

Exocytosis Does Not Generate Calcium Currents

Vesicular calcium channels, if present, could be either voltage-independent Flower channels or VDCCs. We tested these two possibilities by measuring calcium currents (ICa) after and during depolarization, respectively. Depolarization at the calyx was 10 ms from the holding potential of −80 to +10 mV (applies unless mentioned otherwise, depol$_{10ms}$), which induced an ICa of 2.10 ± 0.11 nA and a capacitance jump (ΔCm) of 427 ± 24 fF (n = 12, Figure 1A). At the ΔCm peak, ~400–500 ms after depol$_{10ms}$, the steady-state ICa was undetectable (<3 pA), suggesting that exocytosis did not insert calcium channels to generate steady-state ICa at −80mV. Alternatively, a calcium-dependent outward current could be in balance with the exocytosis-generated ICa. This latter possibility was ruled out because we detected no outward current (<3 pA at 400–500 ms after

depol$_{10ms}$) when the ΔCm was reduced to 83 ± 9 fF (n = 5) or ~19% of control by botulinum neurotoxin E (BoNT/E, 150 nM, in pipette, Figure S1A). Similar results were obtained when BAPTA (10 mM) was included with BoNT/E to block potential calcium-dependent currents (Figure S1B, n = 5).

Because a vesicle's membrane capacitance is ~0.07 fF (Sun et al., 2002; He et al., 2006), the 427 fF ΔCm induced by depol$_{10ms}$ corresponded to ~6,100 vesicles. If each vesicle contained exactly 1 calcium channel, ~6,100 channels would be inserted to the plasma membrane. ICa traces were originally low-pass filtered at 3 kHz (Figure 1A, black). After we low-pass filtered ICa traces at 100 Hz (Figure 1A, red), the SD of ICa traces was 0.83 ± 0.08 pA (n = 8). We then set our detection limit at 3 pA, which was greater than three times the SD with >99.7% confidence for detecting changes every 10 ms. If there were 6,100 channels inserted at the plasma membrane, each channel would generate <0.0005 pA of ICa, ~600 times less than the

A

Rat Flower protein sequence

TM1   TM2

MSGSVAAGAAAGPVPPAQEEGMTWWYRWLCRLAGVLGAVSCAISGLFNCVTIHPLNIAAGVWMIMNAFILLLCEAPFCCQFVEFAN
1   10   20   30   40   50   60   70   80

TM3   TM4

TVAEKVDRLRSWQKAVFYCGMAIVPIVMSLTLTTTLLGNAIAFATGVLYGLSALGKKGDAISYARIQQQRQQADEEKLAETFEGEL
90   100   110   120   130   140   150   160   170

B

C

Flower   vGluT$_1$ superimposed

P9

P9 + Flower peptide

P13

10 µm

D

Flower antibody — 20 kDa

DDK antibody — 20 kDa

no transfection   Flower-DDK transfection

E

Flower

VAMP2

cytosol   SVs

Figure 2. Flower Localization in Rat Brain, Calyces, and Synaptic Vesicles

(A) Rat Flower sequence (NP_001100031.1). Black lines denote the transmembrane domains (TM). Red line denotes the Flower peptide used for Flower antibody generation.

(B) Western blot of Flower and VAMP2 from rat brain.

(C) Confocal images showing the antibody staining against Flower (left) and vGluT$_1$ (middle, calyx labeling) at P9 (upper) and P13 (lower) calyces (right panel is left and middle panels superimposed). Flower peptide preincubation blocked Flower antibody staining of P9 calyces (middle).

(D) Western blot of DDK-tagged Flower protein from HEK293 cells with or without *Flower* transfection.

(E) Western blot of Flower and VAMP2 from cytosol and synaptic vesicles (SVs) purified from rat brain.

single-VDCC current ($\sim$0.3 pA at $-$80mV) (Li et al., 2007; Weber et al., 2010). There was no such small single-channel current observed. If calcium channels with a single-channel current similar to VDCCs (0.3 pA) were in a fraction of vesicles, the fraction would be <0.16% ($\approx$3 pA/0.3 pA/6,100). Thus, fused vesicles did not contain voltage-independent calcium channels with any reported conductance.

Consistent with this conclusion, the volume-averaged [Ca^{2+}]$_i$ detected with fura-2 decayed to within 10 nM above baseline at 2–3 s after depol$_{10ms}$, at which >$\sim$75% ΔCm remained, indicating that fused vesicle membrane could not generate significant [Ca^{2+}]$_i$ increase (n = 5, Figure 1B). Similar results (<10 nM at 2–3 s, n = 4) were observed when endocytosis was blocked by 0.3 mM GDPβS in the pipette.

Two sets of data suggest that exocytosis did not generate ICa during depolarization. First, depol$_{10ms}$ induced a ΔCm 267% ± 13% (n = 6) of that induced by a 2 ms depolarization (Figure 1C). However, ICa during depol$_{10ms}$ did not increase. ICa at 9.9 ms during depolarization was 84% ± 2% (n = 6) of that at 2 ms (Figure 1C). This was not due to a balance between calcium-dependent outward currents and exocytosis-inserted ICa because in the presence of BoNT/E that blocked exocytosis, ICa at 9.9 ms during depolarization was 85% ± 2% (n = 5, Figure S1A, inset) of that at 2 ms, similar to control. Similar results (86% ± 1%, n = 5) were obtained in the presence of BAPTA (10 mM) and BoNT/E that blocked potential calcium-dependent currents (Figure S1B, inset). Second, in control (150 nM boiled BoNT/E in pipette) during ten pulses of 20 ms depolarization at 10 Hz

(depol$_{20ms \times 10}$), the total ΔCm after the first pulse was 503 ± 33 fF but increased by 938 ± 55 fF after the tenth pulse (n = 5), corresponding to fusion of additional $\sim$13,000 ($\approx$938/0.07) vesicles. This additional fusion predicts an increase of 1.3 nA of ICa if each fused vesicle contains a VDCC with reported $\sim$0.1 pA single-channel current at +10mV (Weber et al., 2010). However, ICa decreased from 2.42 ± 0.12 nA at the first pulse to 1.27 ± 0.06 nA (53% ± 3%, n = 5) at the tenth pulse (Figure 1D), suggesting no vesicular VDCCs. This ICa decrease was not due to a balance between ICa inactivation and exocytosis-induced VDCC insertion because a similar ICa decrease was observed in the presence of BoNT/E (150 nM), which blocked the total ΔCm induced by depol$_{20ms \times 10}$ to 179 ± 27 fF ($\sim$12% of control, n = 5, Figures 1E and 1F). Addition of the calcium buffer BAPTA (10 mM) together with BoNT/E (150 nM) partially relieved ICa decrease (Figures S1C and S1D, n = 5), consistent with calcium-dependent ICa inactivation (Forsythe et al., 1998; Xu and Wu, 2005). We concluded that exocytosis did not generate calcium currents during and after depolarization (Figure 1).

Flower at Nerve Terminals

Results in Figure 1 prompted us to determine whether Flower is expressed in rat brain. An antibody we generated against Flower amino acids 151–165 (Figure 2A) detected a major band in rat (P8) brain (Figure 2B). Immunostaining with this antibody was co-localized with the antibody staining against vesicular glutamate transporter 1 (vGluT$_1$), which labeled calyces (Figure 2C, upper). Our antibody is specific to Flower because (1) Flower peptide (Flower amino acids 151–165) blocked Flower antibody staining of the calyx (Figure 2C, middle), and (2) Flower antibody specifically recognized DDK-tagged Flower protein overexpressed in HEK293 cells, which contained no endogenous Flower protein (Figure 2D). The molecular weight of Flower overexpressed in
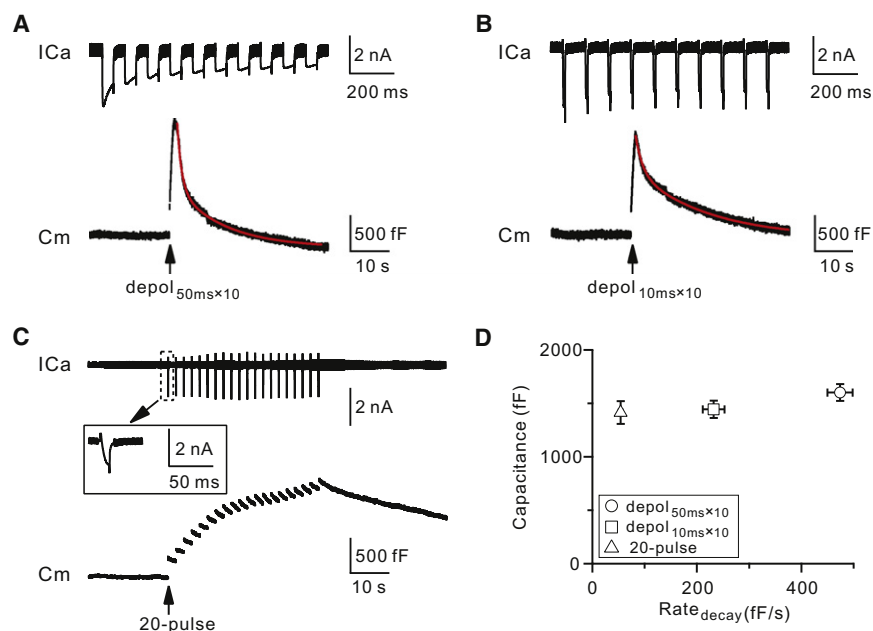
Figure 3. Voltage-Dependent Calcium Currents Determine the Endocytosis Rate

(A–C) Sampled ICa and Cm induced by depol$_{50ms\times10}$ (A), depol$_{10ms\times10}$ (B), and 20 pulse train (C). Red curves are biexponential fit of the capacitance decay (A: τ, 1.1 and 12 s; B: τ, 1.8 and 18.7 s). The inset shows ICa induced by the first pulse (-80 to -5 mV) in the 20 pulse train.

(D) The ΔCm (mean $\pm$ SE) is plotted versus the Rate$_{decay}$ (mean $\pm$ SE) induced by depol$_{50ms\times10}$ (circle, n = 12), depol$_{10ms\times10}$ (square, n = 13), and the 20 pulse train (triangle, n = 18).

See also Figures S2B–S2D.

HEK293 cells ($\sim$20 kDa) was similar to that in *Drosophila* (Yao et al., 2009) but smaller than that in rat brain extracts ($\sim$25 kDa, Figures 2B and 2D), likely due to posttranslational modification in rat brain.

Western blot of proteins from cytosol and synaptic vesicles purified from the whole rat brain showed that Flower was preferentially localized in vesicles, similar to vesicle protein VAMP2 (Figure 2E). These results suggest that Flower is expressed in synaptic vesicles of rat brain and calyces, consistent with the report of *Drosophila* (Yao et al., 2009). Although these results suggest expression of Flower at many synapses, we do not know whether Flower is expressed at all or only a fraction of synapses in the brain. Nevertheless, Flower expression at the calyx and synaptic vesicles (Figure 2), together with the lack of exocytosis-generated ICa (Figure 1), suggests that vesicular Flower insertion to the plasma membrane does not generate ICa.

VDCC, but Not Exocytosis, Determines Endocytosis Rate

To determine whether the plasma membrane VDCC controls endocytosis, we measured endocytosis after different VDCC-mediated ICa charges (QICas) while maintaining similar amounts of exocytosis (similar inserted vesicular proteins). Ten pulses of 50 ms depolarization at 10 Hz (depol$_{50ms\times10}$) induced a ΔCm of 1603 $\pm$ 78 fF (n = 12) and an QICa of 453 $\pm$ 35 pC (n = 12, Figures 3A and 3D). The capacitance decay, which reflects endocytosis, was biexponential with a τ of 1.2 $\pm$ 0.1 s (n = 12; weight, 62% $\pm$ 4%) and 12.5 $\pm$ 0.4 s (n = 12), respectively. The initial decay rate (Rate$_{decay}$) was 474 $\pm$ 24 fF/s (n = 12), which reflected mostly the initial rate of the rapid endocytosis component because the rapid component contributed >80% of the Rate$_{decay}$ after this stimulus (Wu et al., 2009).

Ten pulses of 10 ms depolarization at 10 Hz (depol$_{10ms\times10}$) induced a similar ΔCm (1445 $\pm$ 80 fF, n = 13; p = 0.17) as

depol$_{50ms\times10}$, likely because each 10 or 50 ms depolarization depleted most readily releasable vesicles (Wu and Wu, 2009). Under this condition both depol$_{10ms\times10}$ and depol$_{50ms\times10}$ may cause repeated depletion and replenishment of the readily releasable pool at near maximal speed. Depol$_{10ms\times10}$ induced a much less QICa (193 $\pm$ 14 pC, n = 13; p < 0.01) and Rate$_{decay}$ (231 $\pm$ 21 fF/s, n = 13; p < 0.01) than depol$_{50ms\times10}$ (Figures 3B and 3D). The capacitance decay was biexponential with a τ of 2.1 $\pm$ 0.2 s (n = 13; weight, 31% $\pm$ 4%) and 18.1 $\pm$ 1.0 s (n = 13), respectively (Figure 3B). The τ and the weight of the rapid component were slower and smaller than those induced by depol$_{50ms\times10}$ (p < 0.01). However, the rapid component of endocytosis still contributed to the Rate$_{decay}$ by more than 80% (calculation not shown). Evidently, the Rate$_{decay}$ difference induced by depol$_{50ms\times10}$ and depol$_{10ms\times10}$ is not due to the exocytosis difference (Figures 3A, 3B, and 3D). It must be due to the difference in the VDCC-mediated QICa ($\sim$453 versus $\sim$193 pC) because calcium influx triggers and speeds up endocytosis at calyces (Wu et al., 2009; Hosoi et al., 2009).

Twenty pulses of 10 ms depolarization from -80 to -5mV at 0.5 Hz (20 pulse train) induced a ΔCm (1414 $\pm$ 107 fF, n = 18) similar to those induced by depol$_{10ms\times10}$ or depol$_{50ms\times10}$ (p > 0.1; Figures 3C and 3D), but a much slower endocytosis, reflected as a mono-exponential capacitance decay with a τ >30 s (n = 18) and a much smaller Rate$_{decay}$ (53 $\pm$ 4 fF/s, n = 18, Figures 3C and 3D; p < 0.01). This slower Rate$_{decay}$ was clearly not caused by smaller ΔCm and, thus, not by smaller amount of inserted vesicular proteins (Figure 3D). It was caused by smaller calcium concentration for two reasons. First, each pulse from -80 to -5mV induced an ICa (1.4 $\pm$ 0.1 nA, n = 18; Figure 3C) much smaller than that by depolarization to +10mV during depol$_{10ms\times10}$ (2.2 $\pm$ 0.1 nA, n = 13; p < 0.01). Second, the pulse was repeated at 0.5 Hz, at which calcium summation was negligible compared to the 10 Hz train (Figure 1B).

P/Q-type Calcium Channels Control Endocytosis

To provide more direct evidence that VDCCs couple exo- to endocytosis, we blocked VDCCs with the P/Q-type VDCC blocker, ω-Agatoxin-IVA. Calyces in P7–P10 rats contain
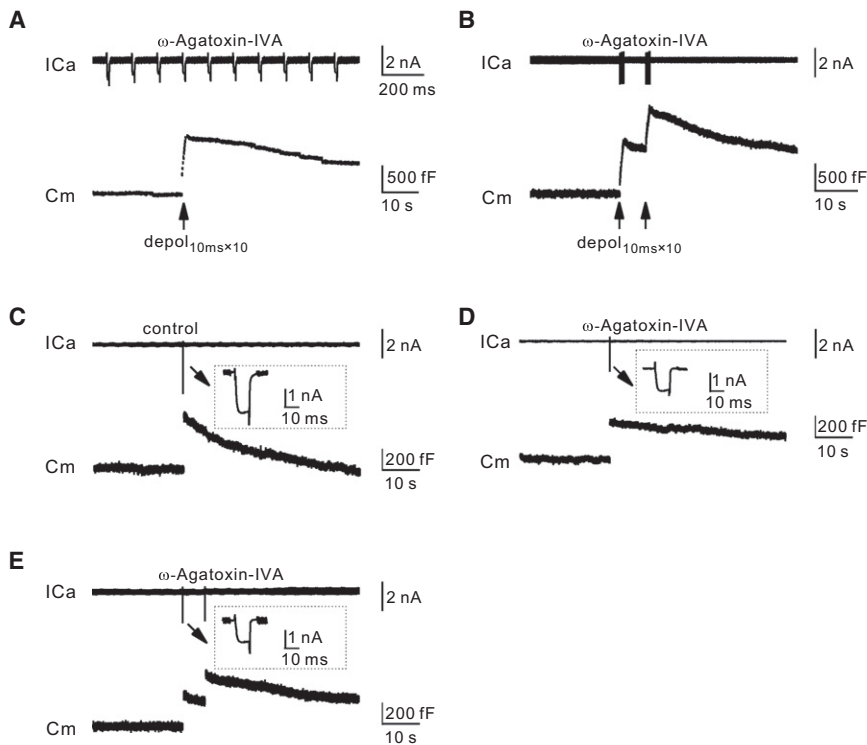
Figure 4. P/Q-type Calcium Channels Are Involved in Rapid and Slow Endocytosis

(A and B) Sampled ICa and Cm induced by a depol$_{10ms×10}$ (A) or a pair of depol$_{10ms×10}$ at 5 s interval (B) in the presence of ω-Agatoxin-IVA (200 nM, bath).

(C–E) Sampled ICa and Cm in the absence (control, C) or the presence of ω-Agatoxin-IVA (200 nM, D and E). The stimulation was a depol$_{10ms}$ in (C) and (D), and a pair of depol$_{10ms}$ in (E).

frequency (0.5 Hz) train generated negligible (nanomolar range) calcium summation at terminals (Figure 1B), whereas more than a few micromolars of calcium are needed to trigger endocytosis at calyces (Wu et al., 2009; Hosoi et al., 2009). Second, ΔCm induced by the 20 pulse train was much higher, which may saturate the endocytosis capacity and thus slow down endocytosis (Sankaranarayanan and Ryan, 2000; Wu et al., 2005).

In the presence of ω-Agatoxin-IVA (200 nM), depol$_{10ms}$ induced a QICa (8.8 ± 0.4 pC, n = 14, Figure 4D; peak amplitude, 0.91 ± 0.06 nA) ∼45% of control (19.5 ± 1.0 pC, n = 12, peak amplitude: 2.10 ± 0.11 nA; Figure 4C), and a ΔCm (270 ± 17 fF, n = 14, Figure 4D) about 63% of control (427 ± 24 fF, n = 12, Figure 4C). The capacitance decay was too slow to fit with an exponential function (Figure 4D). The Rate$_{decay}$ was 16.3 ± 1.6 fF/s (n = 14, Figure 4D), much slower than control (36.7 ± 2.7 fF/s, n = 12, Figure 4C; p < 0.01). The slower Rate$_{decay}$ and endocytosis time course were not caused by the ΔCm decrease because in the presence of ω-Agatoxin-IVA, a pair of depol$_{10ms}$ values at 5 s interval induced a ΔCm (393 ± 27 fF, n = 9; Figure 4E) similar to that by a depol$_{10ms}$ in control (p = 0.31), but a Rate$_{decay}$ (18.7 ± 1.6 fF/s, n = 9; Figure 4E) much slower than that by a depol$_{10ms}$ in control (p < 0.01; Figure 4C). Thus, VDCCs, including P/Q-type, couple exocytosis to slow endocytosis.

Results shown thus far were from P7–P10 rats, in which calyces are not mature. In P13–P14 rats in which calyces are mostly mature (Schneggenburger and Forsythe, 2006), we repeated experiments similar to those shown in Figures 1A and 2C (upper) and Figures 3A and 3B and found similar results (Figure S2; Figure 2C, lower). Thus, our observations applied to both immature and mature calyces.

DISCUSSION

We found that fusion did not generate calcium currents or influx at the plasma membrane (Figure 1), that Flower was localized at synaptic vesicles of rat brain and calyces (Figure 2), and that the current charge of VDCCs at the plasma membrane, including P/Q-type, determined the rate of rapid and slow endocytosis (Figures 3 and 4). These results suggest that fused vesicle

P/Q-, N-, and R-type VDCCs, among which P/Q-type contributes about two-thirds of ICa (Wu et al., 1999; Iwasaki et al., 2000). In the presence of ω-Agatoxin-IVA (200 nM, bath, 10–40 min), depol$_{10ms×10}$ induced a QICa (72 ± 6 pC, n = 12) and a ΔCm (812 ± 41 fF, n = 12; Figure 4A) smaller than control (193 ± 14 pC, 1445 ± 80 fF, n = 13; Figure 3B; p < 0.01). Endocytosis was much slower because the capacitance decay was too slow to fit exponentially, and the Rate$_{decay}$ (50 ± 4 fF/s, n = 12, Figure 4A) was much slower than control (231 ± 21 fF/s, n = 13, Figure 3B; p < 0.01). The slower Rate$_{decay}$ was not due to the ΔCm decrease because a pair of depol$_{10ms×10}$ values at 5 s interval induced a ΔCm (1260 ± 36 fF, n = 10, Figure 4B) similar to that by a depol$_{10ms×10}$ in control (p > 0.05; Figure 3B) but induced a Rate$_{decay}$ (61 ± 5 fF/s, n = 10, Figure 4B) much slower than that by a depol$_{10ms×10}$ in control (p < 0.01; Figure 3B). Thus, VDCCs, including P/Q-type, couple exocytosis to rapid endocytosis.

To study slow endocytosis, depol$_{10ms}$ was applied. Depol$_{10ms}$ induced a ΔCm of 427 ± 24 fF (n = 12), followed by a mono-exponential decay with a τ of 15.8 ± 0.7 s (n = 12) and a Rate$_{decay}$ of 36.7 ± 2.7 fF/s (n = 12, Figure 4C). The τ (∼15.8 s) of this slow endocytosis was much shorter than that after the 20 pulse train, which also induced slow endocytosis with a τ >30 s (n = 18; Figure 3C), but a ΔCm ∼231% higher than that induced by depol$_{10ms}$. Thus, more exocytosis was followed by endocytosis with a slower τ, inconsistent with the vesicular channel hypothesis. The slower τ was likely due to two factors. First, ICa (1.4 ± 0.1 nA, n = 18) induced by each pulse during the 20 pulse train was less than that induced by a depol$_{10ms}$ (2.10 ± 0.11 nA, n = 12; p < 0.01). Although there were 20 pulses, the low-

membrane and proteins, including Flower, could not generate calcium currents to initiate endocytosis. Instead, plasma membrane VDCCs, including P/Q-type, couple exocytosis to two widely observed forms of endocytosis: rapid and slow endocytosis.

Our findings are different from a study showing that vesicular VDCCs inserted at the plasma membrane via exocytosis are required for endocytosis in sea urchin eggs (Smith et al., 2000). The difference is likely due to the significant differences of the two systems. Calyces are nerve terminals containing small ($\sim$50 nm) vesicles with endocytosis lasting for less than tens of seconds (Figures 3 and 4), whereas sea urchin eggs contain very large ($\sim$1 μm) vesicles with endocytosis lasting for $\sim$15–30 min.

Our findings are different from the study of *Drosophila* synapses (Yao et al., 2009). Although the synapse specificity could provide an explanation, the Flower hypothesis is not well established as discussed below. At *Drosophila* nerve terminals, vesicular Flower insertion into the plasma membrane via exocytosis increases the $[Ca^{2+}]_i$ at the submicromolar range after prolonged tetanic stimulation (Yao et al., 2009), whereas endocytosis at nerve terminals is initiated by more than a few micromolars of calcium (Wu et al., 2009; Hosoi et al., 2009; Beutner et al., 2001). Furthermore, the time course of the calcium rise via Flower channels is in the order of 10–60 min (Yao et al., 2009), which was too slow to initiate endocytosis that typically lasts for a few to tens of seconds at many synapses, including *Drosophila* synapses (Poskanzer et al., 2003; Wu et al., 2007). Such slow calcium permeation might explain why we did not detect calcium currents or influx within a few seconds after exocytosis.

Endocytosis quantified with FM1-43 uptake at one time point after prolonged (1 min) high potassium stimulation was reduced by $\sim$41% in Flower mutants (Yao et al., 2009). Compared to a complete block of endocytosis by calcium buffers (Wu et al., 2009; Hosoi et al., 2009; Yamashita et al., 2010), such a small defect suggests that Flower is not essential in initiating endocytosis. Furthermore, whether Flower plays a role under physiological conditions is unclear because endocytosis after brief physiological depolarization was not quantified in Flower mutants (Yao et al., 2009).

Although the Flower hypothesis is not well established, the present work firmly established a critical role of plasma membrane VDCCs, but not vesicular channels, in initiating and speeding up endocytosis at calyces. Whether our results apply to other synapses has not been tested. However, except that the calyx is much larger than conventional boutons, it is similar to other nerve terminals in many aspects, such as the active zone size, the vesicle number per active zone, short-term plasticity, transmitter release properties, calcium currents, and endocytosis time course (Schneggenburger and Forsythe, 2006; Wu et al., 2007; Xu et al., 2007). Our findings are, therefore, likely to apply to other synapses. Considering that VDCCs control exocytosis in all chemical synapses and many non-neuronal secretory cells, we suggest that VDCC-mediated exo-endocytosis coupling is a common mechanism at synapses and many non-neuronal secretory cells. Consistent with this suggestion, calcium influx was found to regulate endocytosis at many synapses and non-neuronal secretory cells (Ceccarelli

and Hurlbut, 1980; Marks and McMahon, 1998; Cousin and Robinson, 1998; Gad et al., 1998; Sankaranarayanan and Ryan, 2001; Balaji et al., 2008; Neves et al., 2001; Clayton et al., 2007; Artalejo et al., 1995; He et al., 2008).

EXPERIMENTAL PROCEDURES

Slice preparation and capacitance recordings were described previously by Sun and Wu (2001) and Sun et al. (2004). Briefly, parasagittal brain stem slices (200 μm thick) containing the medial nucleus of the trapezoid body were prepared from Wistar rats using a vibratome. Unless mentioned, rat age was 7–10 days old. All animal protocols followed the guidelines of the National Institutes of Health, USA. Whole-cell capacitance measurements were made with the EPC-10 amplifier together with the software lock-in amplifier (PULSE, HEKA, Lambrecht, Germany) that implements Lindau-Neher's technique. The frequency of the sinusoidal stimulus was 1,000 Hz, and the peak-to-peak voltage of the sine wave was $\leq$60mV. We pharmacologically isolated presynaptic ICa with a bath solution ($\sim$22°C–24°C) containing 105 mM NaCl, 20 mM TEA-Cl, 2.5 mM KCl, 1 mM MgCl$_2$, 2 mM CaCl$_2$, 25 mM NaHCO$_3$, 1.25 mM NaH$_2$PO$_4$, 25 mM glucose, 0.4 mM ascorbic acid, 3 mM *myo*-inositol, 2 mM sodium pyruvate, 0.001 mM tetrodotoxin (TTX), 0.1 mM 3,4-diaminopyridine (pH 7.4) when bubbled with 95% O$_2$ and 5% CO$_2$. When ω-Agatoxin-IVA was applied to the bath, cytochrome c (0.1 mg/ml) was also included. The presynaptic pipette (3.5–5 MΩ) solution contained 125 mM Cs-gluconate, 20 mM CsCl, 4 mM MgATP, 10 mM Na$_2$-phosphocreatine, 0.3 mM GTP, 10 mM HEPES, 0.05 mM BAPTA (pH 7.2) adjusted with CsOH.

The statistical test was a t test. Means are presented as $\pm$ SE. Rate$_{decay}$ was measured from 0.3 s to 3 or 6 s after stimulation (Wu et al., 2009). The $[Ca^{2+}]_i$ was measured with fura-2 (50 μM, replacing BAPTA in the pipette), the Olympus upright epifluorescence microscope (BX51WI, LumplanFI 40$\times$, n.a. 0.8), a polychromatic illumination system (T.I.L.L. Photonics, Munich), and a photodiode for fluorescence recording (Xu and Wu, 2005).

Cytosol and synaptic vesicle proteins were prepared by sucrose gradient fractionation (Yao et al., 2009). P8 rat brain was homogenized and centrifuged to yield a crude synaptosomal pellet, which was then resuspended in 100 mM NaCl, 20 mM HEPES (pH 7.4) solution and loaded onto sucrose step gradient (0.2–0.4 M) for centrifugation (20,000 $\times$ g, 5 hr). Synaptic vesicles were collected from 0.2 to 0.4 M sucrose interface. The proteins were quantified and subject to SDS-PAGE for western blot assay (Invitrogen).

For western blot, P8 rat brain was homogenized and centrifuged to yield supernatants, which were quantified and loaded to SDS-PAGE for immunoblotting using a custom-made rabbit antibody against Flower (1:50; GenScript) and a mouse antibody against VAMP2 (1:10,000; Synaptic Systems).

For immunohistochemistry, rats were anesthetized by Nembutal, fixed by paraformaldehyde, and infiltrated with 30% sucrose. OCT (Electron Microscopy Sciences)-embedded rat brain was sectioned using a cryostat (Leica CM3050S) at 30 μm thickness. The calyces were recognized by a guinea pig antibody against vGluT$_1$ (1:5,000; Millipore), and Flower proteins at calyces were identified using the rabbit antibody against Flower (1:50; GenScript). For the peptide-blocking experiment (Figure 2C, middle), Flower antibody was preincubated with the Flower peptide (Figure 2A, red) overnight at 4°C. Dylight-488 donkey anti-rabbit and rhodamine-conjugated donkey anti-guinea pig antibodies (1:100; Jackson ImmunoResearch Laboratories) were used as secondary antibodies. Images were collected by Zeiss LSM510 confocal microscopy (40$\times$, N/A 1.3).

SUPPLEMENTAL INFORMATION

Supplemental Information includes two figures and can be found with this article online at doi:10.1016/j.celrep.2012.04.011.

LICENSING INFORMATION

REFERENCES

Artalejo, C.R., Henley, J.R., McNiven, M.A., and Palfrey, H.C. (1995). Rapid endocytosis coupled to exocytosis in adrenal chromaffin cells involves Ca2+, GTP, and dynamin but not clathrin. Proc. Natl. Acad. Sci. USA *92*, 8328–8332.

Balaji, J., Armbruster, M., and Ryan, T.A. (2008). Calcium control of endocytic capacity at a CNS synapse. J. Neurosci. *28*, 6742–6749.

Beutner, D., Voets, T., Neher, E., and Moser, T. (2001). Calcium dependence of exocytosis and endocytosis at the cochlear inner hair cell afferent synapse. Neuron *29*, 681–690.

Brose, N., and Neher, E. (2009). Flowers for synaptic endocytosis. Cell *138*, 836–837.

Ceccarelli, B., and Hurlbut, W.P. (1980). Ca^{2+}-dependent recycling of synaptic vesicles at the frog neuromuscular junction. J. Cell Biol. *87*, 297–303.

Clayton, E.L., Evans, G.J., and Cousin, M.A. (2007). Activity-dependent control of bulk endocytosis by protein dephosphorylation in central nerve terminals. J. Physiol. *585*, 687–691.

Cousin, M.A., and Robinson, P.J. (1998). Ba^{2+} does not support synaptic vesicle retrieval in rat cerebrocortical synaptosomes. Neurosci. Lett. *253*, 1–4.

Forsythe, I.D., Tsujimoto, T., Barnes-Davies, M., Cuttle, M.F., and Takahashi, T. (1998). Inactivation of presynaptic calcium current contributes to synaptic depression at a fast central synapse. Neuron *20*, 797–807.

Gad, H., Löw, P., Zotova, E., Brodin, L., and Shupliakov, O. (1998). Dissociation between Ca^{2+}-triggered synaptic vesicle exocytosis and clathrin-mediated endocytosis at a central synapse. Neuron *21*, 607–616.

He, L., Wu, X.S., Mohan, R., and Wu, L.G. (2006). Two modes of fusion pore opening revealed by cell-attached recordings at a synapse. Nature *444*, 102–105.

He, Z., Fan, J., Kang, L., Lu, J., Xue, Y., Xu, P., Xu, T., and Chen, L. (2008). Ca2+ triggers a novel clathrin-independent but actin-dependent fast endocytosis in pancreatic beta cells. Traffic *9*, 910–923.

Hosoi, N., Holt, M., and Sakaba, T. (2009). Calcium dependence of exo- and endocytotic coupling at a glutamatergic synapse. Neuron *63*, 216–229.

Iwasaki, S., Momiyama, A., Uchitel, O.D., and Takahashi, T. (2000). Developmental changes in calcium channel types mediating central synaptic transmission. J. Neurosci. *20*, 59–65.

Kuo, S.P., and Trussell, L.O. (2009). A new ion channel blooms at the synapse. Neuron *63*, 566–567.

Leitz, J., and Kavalali, E.T. (2011). Ca^{2+} influx slows single synaptic vesicle endocytosis. J. Neurosci. *31*, 16318–16326.

Li, L., Bischofberger, J., and Jonas, P. (2007). Differential gating and recruitment of P/Q-, N-, and R-type Ca2+ channels in hippocampal mossy fiber boutons. J. Neurosci. *27*, 13420–13429.

Marks, B., and McMahon, H.T. (1998). Calcium triggers calcineurin-dependent synaptic vesicle recycling in mammalian nerve terminals. Curr. Biol. *8*, 740–749.

Neves, G., Gomis, A., and Lagnado, L. (2001). Calcium influx selects the fast mode of endocytosis in the synaptic terminal of retinal bipolar cells. Proc. Natl. Acad. Sci. USA *98*, 15282–15287.

Poskanzer, K.E., Marek, K.W., Sweeney, S.T., and Davis, G.W. (2003). Synaptotagmin I is necessary for compensatory synaptic vesicle endocytosis in vivo. Nature *426*, 559–563.

Royle, S.J., and Lagnado, L. (2003). Endocytosis at the synaptic terminal. J. Physiol. *553*, 345–355.

Sankaranarayanan, S., and Ryan, T.A. (2000). Real-time measurements of vesicle-SNARE recycling in synapses of the central nervous system. Nat. Cell Biol. *2*, 197–204.

Sankaranarayanan, S., and Ryan, T.A. (2001). Calcium accelerates endocytosis of vSNAREs at hippocampal synapses. Nat. Neurosci. *4*, 129–136.

Schneggenburger, R., and Forsythe, I.D. (2006). The calyx of Held. Cell Tissue Res. *326*, 311–337.

Schweizer, F.E., and Ryan, T.A. (2006). The synaptic vesicle: cycle of exocytosis and endocytosis. Curr. Opin. Neurobiol. *16*, 298–304.

Shupliakov, O., and Brodin, L. (2010). Recent insights into the building and cycling of synaptic vesicles. Exp. Cell Res. *316*, 1344–1350.

Smith, R.M., Baibakov, B., Ikebuchi, Y., White, B.H., Lambert, N.A., Kaczmarek, L.K., and Vogel, S.S. (2000). Exocytotic insertion of calcium channels constrains compensatory endocytosis to sites of exocytosis. J. Cell Biol. *148*, 755–767.

Sun, J.Y., and Wu, L.G. (2001). Fast kinetics of exocytosis revealed by simultaneous measurements of presynaptic capacitance and postsynaptic currents at a central synapse. Neuron *30*, 171–182.

Sun, J.Y., Wu, X.S., and Wu, L.G. (2002). Single and multiple vesicle fusion induce different rates of endocytosis at a central synapse. Nature *417*, 555–559.

Sun, J.Y., Wu, X.S., Wu, W., Jin, S.X., Dondzillo, A., and Wu, L.G. (2004). Capacitance measurements at the calyx of Held in the medial nucleus of the trapezoid body. J. Neurosci. Methods *134*, 121–131.

Vogel, S.S. (2009). Channeling calcium: a shared mechanism for exocytosis-endocytosis coupling. Sci. Signal. *2*, pe80.

von Gersdorff, H., and Matthews, G. (1994). Inhibition of endocytosis by elevated internal calcium in a synaptic terminal. Nature *370*, 652–655.

Weber, A.M., Wong, F.K., Tufford, A.R., Schlichter, L.C., Matveev, V., and Stanley, E.F. (2010). N-type Ca2+ channels carry the largest current: implications for nanodomains and transmitter release. Nat. Neurosci. *13*, 1348–1350.

Wu, L.G., Westenbroek, R.E., Borst, J.G., Catterall, W.A., and Sakmann, B. (1999). Calcium channel types with distinct presynaptic localization couple differentially to transmitter release in single calyx-type synapses. J. Neurosci. *19*, 726–736.

Wu, L.G., Ryan, T.A., and Lagnado, L. (2007). Modes of vesicle retrieval at ribbon synapses, calyx-type synapses, and small central synapses. J. Neurosci. *27*, 11793–11802.

Wu, W., Xu, J., Wu, X.S., and Wu, L.G. (2005). Activity-dependent acceleration of endocytosis at a central synapse. J. Neurosci. *25*, 11676–11683.

Wu, X.S., and Wu, L.G. (2009). Rapid endocytosis does not recycle vesicles within the readily releasable pool. J. Neurosci. *29*, 11038–11042.

Wu, X.S., McNeil, B.D., Xu, J., Fan, J., Xue, L., Melicoff, E., Adachi, R., Bai, L., and Wu, L.G. (2009). Ca(2+) and calmodulin initiate all forms of endocytosis during depolarization at a nerve terminal. Nat. Neurosci. *12*, 1003–1010.

Xu, J., and Wu, L.G. (2005). The decrease in the presynaptic calcium current is a major cause of short-term depression at a calyx-type synapse. Neuron *46*, 633–645.

Xu, J., He, L., and Wu, L.G. (2007). Role of Ca(2+) channels in short-term synaptic plasticity. Curr. Opin. Neurobiol. *17*, 352–359.

Yamashita, T., Eguchi, K., Saitoh, N., von Gersdorff, H., and Takahashi, T. (2010). Developmental shift to a mechanism of synaptic vesicle endocytosis requiring nanodomain Ca2+. Nat. Neurosci. *13*, 838–844.

Yao, C.K., Lin, Y.Q., Ly, C.V., Ohyama, T., Haueter, C.M., Moiseenkova-Bell, V.Y., Wensel, T.G., and Bellen, H.J. (2009). A synaptic vesicle-associated Ca2+ channel promotes endocytosis and couples exocytosis to endocytosis. Cell *138*, 947–960.